

Novel Hinge Binder Improves Activity and Pharmacokinetic Properties of BRAF Inhibitors

Alfonso Zambon,[†] Delphine Ménard,[†] Bart M. J. M. Suijkerbuijk,[†] Ion Niculescu-Duvaz,[†] Steven Whittaker,[‡] Dan Niculescu-Duvaz,[‡] Arnaud Nourry,[†] Lawrence Davies,[†] Helen A. Manne,[†] Filipa Lopes,[†] Natasha Preece,[†] Douglas Hedley,[†] Lesley M. Ogilvie,[†] Ruth Kirk,[‡] Richard Marais,[‡] and Caroline J. Springer^{*†}

[†]The Institute of Cancer Research, Cancer Research UK Centre for Cancer Therapeutics, 15 Cotswold Road, Sutton, Surrey SM2 5NG, United Kingdom, and [‡]The Institute of Cancer Research, Cancer Research UK Centre for Cell and Molecular Biology, 237 Fulham Road, London SW3 6JB, United Kingdom

Received March 26, 2010

Mutated BRAF serine/threonine kinase is implicated in several types of cancer, with particularly high frequency in melanoma and colorectal carcinoma. We recently reported on the development of BRAF inhibitors based on a tripartite A–B–C system featuring an imidazo[4,5]pyridin-2-one group hinge binder. Here we present the design, synthesis, and optimization of a new series of inhibitors with a different A–B–C system that has been modified by the introduction of a range of novel hinge binders (A ring). The optimization of the hinge binding moiety has enabled the development of compounds with low nanomolar potencies in both BRAF inhibition and cellular assays. These compounds display optimal pharmacokinetic properties that warrant further in vivo investigations.

Introduction

BRAF^a is a member of the RAF protein kinase family that includes ARAF and CRAF (also known as RAF1). RAF kinases are components of the mitogen-activated protein kinase (MAPK) RAF-MEK-ERK signal transduction cascade, a pathway that regulates several cell functions from proliferation, and survival to differentiation and senescence. Activation of this pathway is a driver in several types of cancers,¹ and large-scale genomic screens have detected mutations of BRAF in malignant melanomas (50%), colorectal cancers (15%), thyroid cancer (30%), and ovarian cancer (30%) and at lower frequencies in several other cancer types.^{2,3} Over 100 mutations have been identified in BRAF, but the most common is a glutamic acid for valine substitution at position 600 (V600E). This single mutation accounts for over 90% of BRAF mutations in cancer, confers 500-fold activation⁴ in melanoma, and has been shown to stimulate cell proliferation and survival.^{4–6} Importantly, inhibition of BRAF blocks proliferation, induces apoptosis in vitro, and blocks tumor growth in vivo,^{6,7} validating BRAF as a therapeutic target in human cancer. Several drug development programs for the treatment of mutant BRAF-driven malignancies have been initiated, with compounds such as PLX4032⁸ (structure not disclosed), *N*-(4-chloro-3-(trifluoromethyl)phenyl)-1-methyl-5-(2-(5-(trifluoromethyl)-1*H*-imidazol-2-yl)pyridin-4-yloxy)-1*H*-benzo[*d*]imidazol-2-amine (RAF265),⁹ (*E*)-5-(2-(4-(2-(dimethylamino)ethoxy)phenyl)-4-(pyridin-4-yl)-1*H*-imidazol-5-yl)-2,3-dihydro-1*H*-inden-1-one oxime (SB590885),¹⁰ and XL281¹¹ (structure not

disclosed), some of which are currently being evaluated in late stage clinical trials.

We have developed a range of V600E BRAF inhibitors,^{12–15} targeting the inactive conformation of V600E BRAF. These type II¹⁶ inhibitors use a common scaffold that comprises a 2,3-dihydroimidazo[4,5]pyridin-2-one moiety binding to the hinge region of BRAF, a meta or para substituted aromatic system occupying the lipophilic DFG-out pocket, a linker interacting with the salt bridge formed between residues Glu501 and Lys483, and a terminal aromatic group (phenyl or pyrazole) that fills the allosteric pockets created by the displacement of the DFG loop. For clarity, we designated the hinge binder, the middle ring, and the terminal aromatic group as rings A, B and C, respectively, and the salt bridge binder as the BC linker.

The pyridoimidazolone moiety was envisaged as having two functions: (1) to afford additional H-bond interactions with the hinge backbone (one from the pyridine nitrogen H-bond acceptor and one via the 3-NH donor of the imidazolone) compared to compounds such as sorafenib, which has a single H-bond from the pyridyl ring, and (2) to improve the PK properties by reducing the number of rotatable bonds.¹² The structure and activities of sorafenib (the multikinase drug designed to be a CRAF inhibitor) and relevant compounds **5a** and **5q** were previously disclosed¹² and are reported in Figure 1. Interestingly, compound **5a** from ref 12, an analogue of sorafenib bearing the alternative pyridoimidazolone hinge binder, has an activity comparable to that of sorafenib (V600E BRAF IC₅₀ of 23 nM vs 43 nM). Furthermore, the removal of the H-bond donor of the pyridoimidazolone moiety by methylation on the 3 position (compound **5q** of ref 12) affects activity only marginally, decreasing it to the level of sorafenib.

This behavior suggests that the H-bond formed between the hinge region and NH group of the imidazolone ring is not optimal. Indeed, docking of compound **5a** from ref 12 into the

*To whom correspondence should be addressed. Phone: +44 20 8722 4214. Fax: +44 20 8722 4046. E-mail: caroline.springer@icr.ac.uk.

^a Abbreviations: Boc, *tert*-butoxycarbonyl; BRAF, V-RAF murine sarcoma viral oncogene homologue B1; ERK, extracellular regulated kinase; MAPK, mitogen-activated protein kinase; MEK, mitogen-activated protein/extracellular regulated kinase; PK, pharmacokinetics; RAF, rapidly growing fibrosarcoma; SAR, structure–activity relationship; THF, tetrahydrofuran.

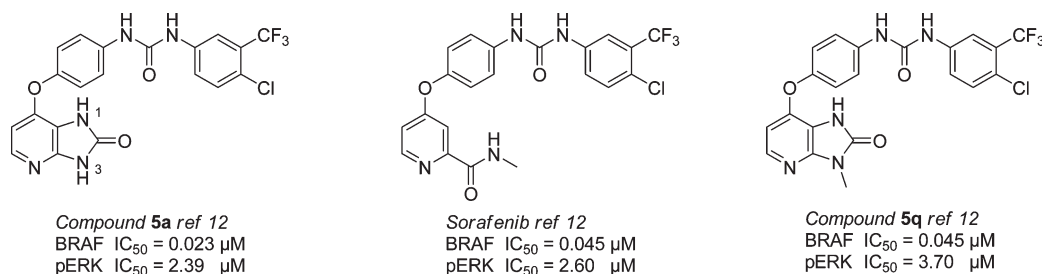


Figure 1. Structural formulas and biological data of sorafenib and compounds **5a** and **5q** from ref 12.

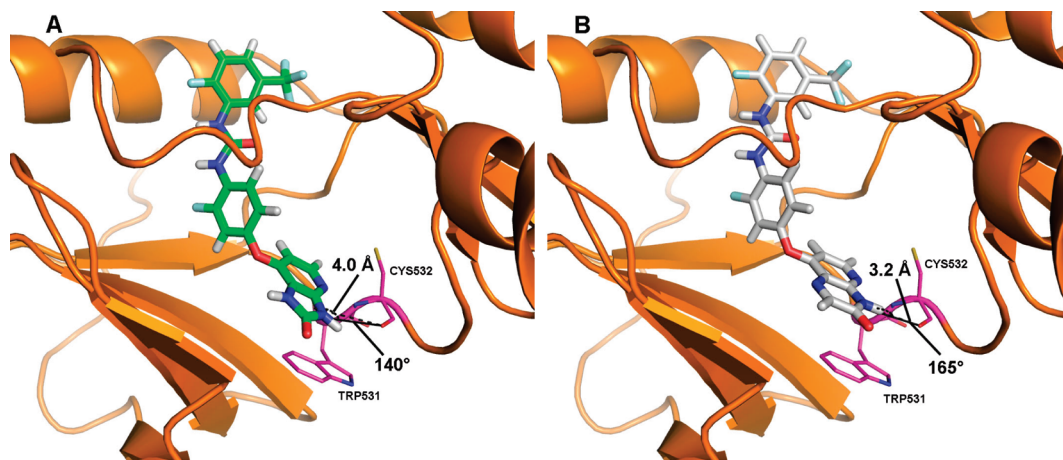


Figure 2. Docking poses of compounds **21r** from ref 13 (A) and **1a** (B) on BRAF.

BRAF/sorafenib cocrystal structure (PDB code UWH)⁴ indicates how, while the nitrogen atom of the pyridine ring forms a strong H-bond with the backbone NH group of Cys532, the geometry of the H-bond interaction between the NH group of the imidazolone moiety and the backbone carbonyl group of Cys532 is far from optimal, at a N–O distance of 4.0 Å and an N–H–O angle of 140° (Figure 2A). Thus, modifying the structure of the pyrimidazolone hinge binder could allow the H-bond donor of the bicyclic ring moiety to form a more favorable interaction with the backbone, enhancing the inhibitory potency toward BRAF. Furthermore, the terminal carbonyl group of the pyrimidazolone group points toward the solvent, and it can be used to fine-tune the PK and solubility properties of the series.

By use of this rationale, alternative hinge binders were explored in order to improve further the affinity for BRAF. Thus, a series of ligands bearing a variety of alternative hinge binders as ring A and a standard B–C system were docked into the BRAF/sorafenib cocrystal structure (PDB code UWH),⁴ and their binding modes were examined in comparison to that of the corresponding pyridoimidazolone inhibitor. A number of these compounds were then synthesized and their activities and PK properties assessed. Here we describe the synthesis of these target compounds and the ensuing structure–activity relationship (SAR) studies.

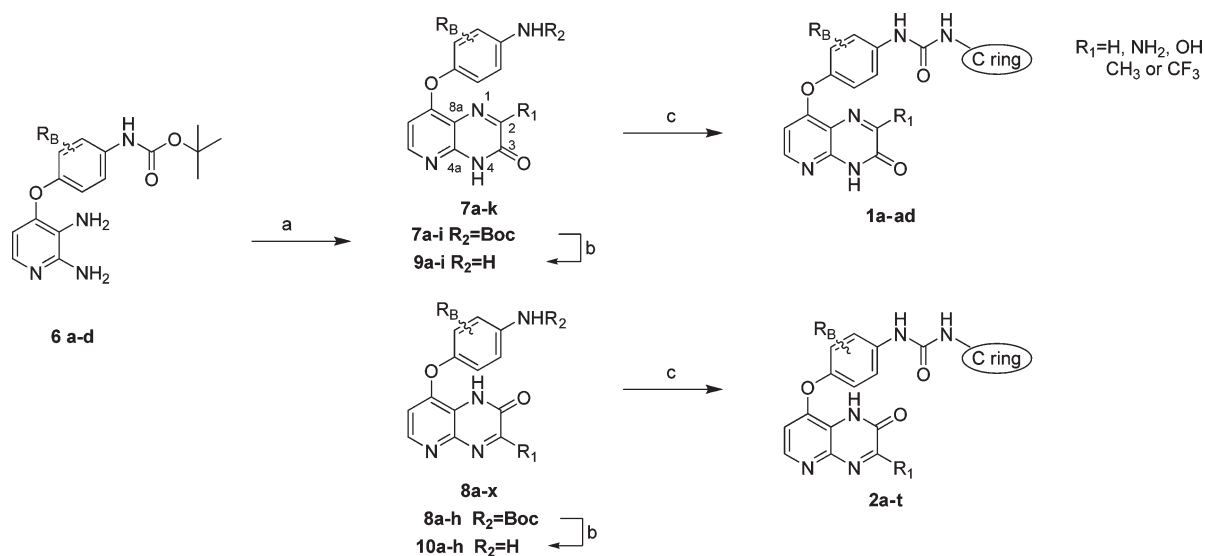
Design and Synthesis

Alternative bicyclic A rings formed by a pyridine fused with a range of five- and six-membered rings bearing H-bond donor and acceptor groups in various patterns were first evaluated through docking on the BRAF/sorafenib cocrystal structure. Among the structures considered, the pyrido[2,3-*b*]pyrazin-3(4*H*)-one group is of particular interest, as the extension of the second ring of the bicyclic system to a six-membered

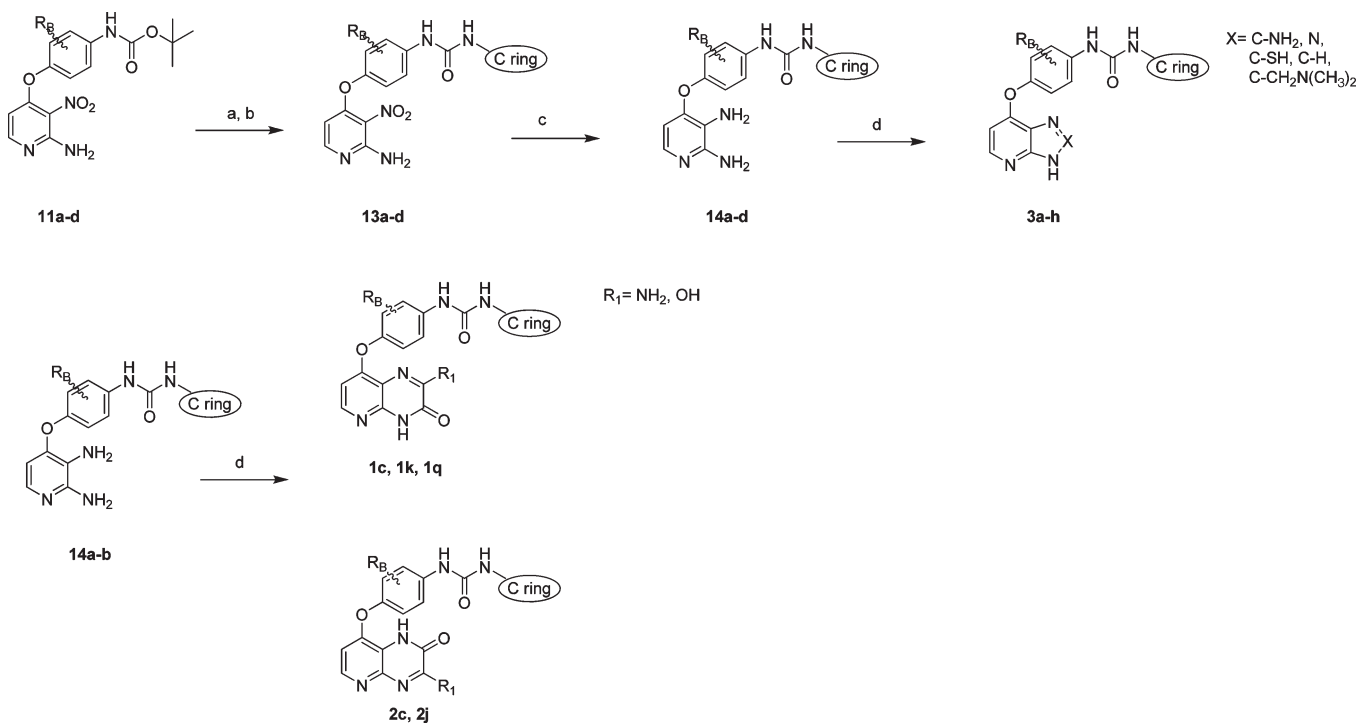
cycle moves the lactam moiety of the inhibitor closer to the carbonyl group of Cys532, while maintaining the H-bond between the pyridine ring and the amide moiety of Cys532 (Figure 2). Also, the pyrido[2,3-*b*]pyrazin-3(4*H*)-one group presents a single H-bond donor versus the two H-bond donors of the pyridoimidazolone moiety, a feature that is expected to improve the PK properties and cell permeability of the scaffold.

The new analogues were synthesized according to the synthetic routes outlined in Schemes 1–3. The target compounds could be accessed either by forming the A–B ring system first and then coupling the terminal group of the B ring to introduce the linker/C ring group as in Scheme 1 and Scheme 3 or, as in Scheme 2, by linking the C ring with the system formed by the B ring and the nitro-amino-pyridine moiety as a precursor of the A ring.¹² The nitro group is then reduced and the resulting diamino compound is condensed with an appropriate dielectrophile to form the target bicyclic A ring. This second route, which requires a single step from the common intermediate to the final product, is particularly suitable for exploring a range of different A ring systems in a parallel fashion and has been used to access A ring systems formed by a pyridine fused to five-membered heterocycles.

The synthesis of compounds **1a–ad** and **2a–t**, featuring a substituted pyridopyrazinone unit, is outlined in Scheme 1. Fused bicyclic systems are obtained by reaction of the already reported diamino intermediates **6a–d**^{12,13} with the appropriate α -keto esters as electrophiles or with ethyl 2-ethoxy-2-iminoacetate in the case of aminopyridopyrazinone compounds **1c**, **1k**, **1w**, **1aa**, **1ad** and **2c**, **2j**, **2p**, **2t**. In the condensation reaction both the pyridopyrazin-2(1*H*)-one and the pyridopyrazin-3(4*H*)-one isomers are obtained and are then separated by chromatography. Removal of the Boc protecting group with tetrabutylammonium fluoride in refluxing THF¹⁷ affords the

Scheme 1. Synthesis of Pyridopyrazinone BRAF Inhibitors **1a–ad** and **2a–t**^a

^a Reagents and conditions: (a) dry EtOH. For $R_1 = \text{H}$: ethyl glyoxylate (50% in toluene). For $R_1 = \text{CH}_3$: ethyl pyruvate. For $R_1 = \text{NH}_2$: ethyl carboethoxyformimidate hydrochloride. For $R_1 = \text{CF}_3$: ethyl trifluoropyruvate. For $R_1 = \text{OH}$: diethyl oxalate, microwave conditions (180 °C, 150W). (b) 1 M TBAF in THF, reflux. (c) Isocyanates, dry DMSO, Ar atm, room temp.

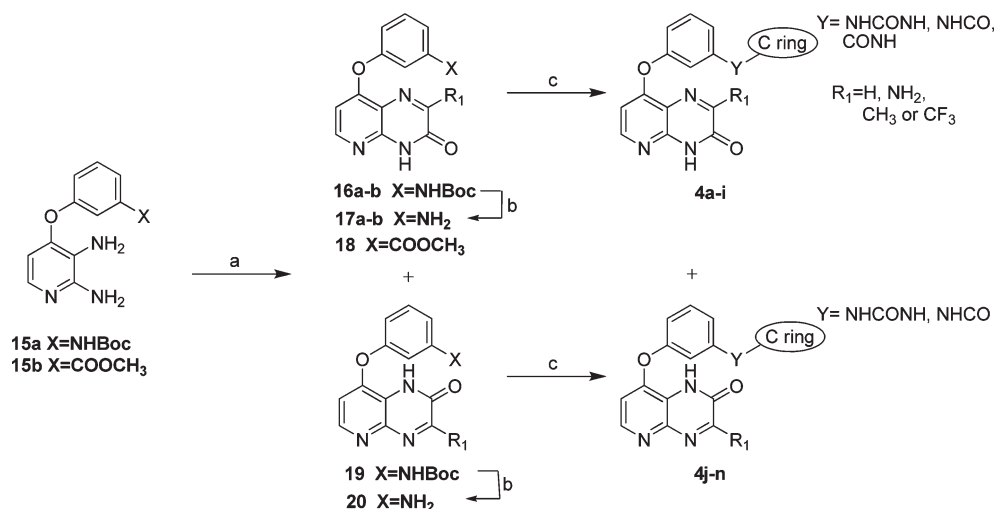
Scheme 2. Synthesis of Compounds **3a–h**^a

^a Reagents and conditions: (a) TFA (only for **11b**); (b) isocyanate, dry THF, Ar; (c) H_2 , 10% Pd/C (d); for $X = \text{N}$ isoamyl nitrite; for $X = \text{C-SH}$ carbon disulfide; for $X = \text{CH}$ ethyl orthoformate; for $X = \text{C-NMe}_2$ *N*-(dichloromethylene)-*N*-methylmethanaminium chloride; $X = \text{C-CH}_2\text{NMe}_2$, $X = 2$ -chloro-1,1,1-triethoxyethane, then dimethylamine.

common intermediates **9a–i** and **10a–h**, which are reacted with the appropriate isocyanate to yield the final urea compounds (Scheme 1). The regiochemistry of the two isomers **8a** and **7a** was assigned by NMR HMBC experiments by the ^1H – ^{13}C coupling between H3 and junction carbon C4a and between H2 and junction carbon C8a, respectively; furthermore, the structure of **8b** was confirmed by X-ray crystallography (see Supporting Information for X-ray data). Assignments of isomers **7b–i** and **8b–h** was made by analogy because of the characteristic

chemical shifts of N4–H protons for isomers **7b–i** and N1–H protons for isomers **8b–h**.

Compounds **3a–h**, regioisomers **1c/2c** and **1k/2j**, and dike-to compound **1q** were synthesized according to Scheme 2; in this case the starting materials are Boc-protected amines **11a–d**. The Boc protecting group is removed as described above, and the free amino moiety of the ring is reacted with 1-fluoro-4-trifluoromethylphenyl isocyanate or 3-*tert*-butyl-1-phenyl-1*H*-pyrazole isocyanate to give ureas **13a–d**. The

Scheme 3. Synthesis of Meta-Substituted Pyridopyrazinone BRAF Inhibitors **4a–n**^a

^a Reagents and conditions: (a) dry EtOH. For $R_1 = \text{H}$: ethyl glyoxylate (50% in toluene). For $R_1 = \text{CH}_3$: ethyl pyruvate. (b) 1 M TBAF in THF, reflux. (c) Isocyanates, dry DMSO, Ar atm, room temp.

nitro group of the pyridine ring is then reduced by catalytic hydrogenation to diamino intermediates **14a–d**, and condensation with the corresponding electrophiles forms the bicyclic A ring system.

The synthesis of meta compounds **4a–n** was carried out according to Scheme 3, following synthetic routes we recently presented for analogous compounds.¹⁴ Thus, compounds **4a–m** were obtained by condensation of diamino compound **15a**¹⁴ with the appropriate electrophiles as described above, followed by deprotection of the NHBoc group and reaction with isocyanate or acyl chloride to give the corresponding ureas or amides. Compound **4n**, bearing a reverse amide linker, was obtained using 3-methoxy benzoate **15b** as starting material. The pyridopyrazin-2(1*H*)-one moiety is then introduced as described above, and the coupling with aminophenylpyrazole was carried out in the presence of trimethylaluminum¹⁸ as coupling agent.

Importantly, pyridopyrazinones are more amenable to chemical manipulation with respect to the pyridoimidazole moiety previously presented. In particular, the endocyclic double bond of final compounds **11** and **2d** can be hydrogenated by sodium borohydride (compounds **5a,b**) directly, while the carbonyl group of the pyrazinone of intermediate **7b** can be converted to the corresponding chloropyrazine by a formal chloro dehydroxylation with *N*-chlorosuccinimide and PPh_3 in 1,4-dioxane at reflux.¹⁹ The resulting chloropyrazine **21** can be synthetically elaborated through nucleophilic aromatic substitution by reaction with amines, allowing the introduction of solubilizing groups on the pyridopyrazinone scaffold, which followed by deprotection and coupling with the appropriate isocyanate gives compounds **5c–k** (Scheme 4).

Results and Discussion

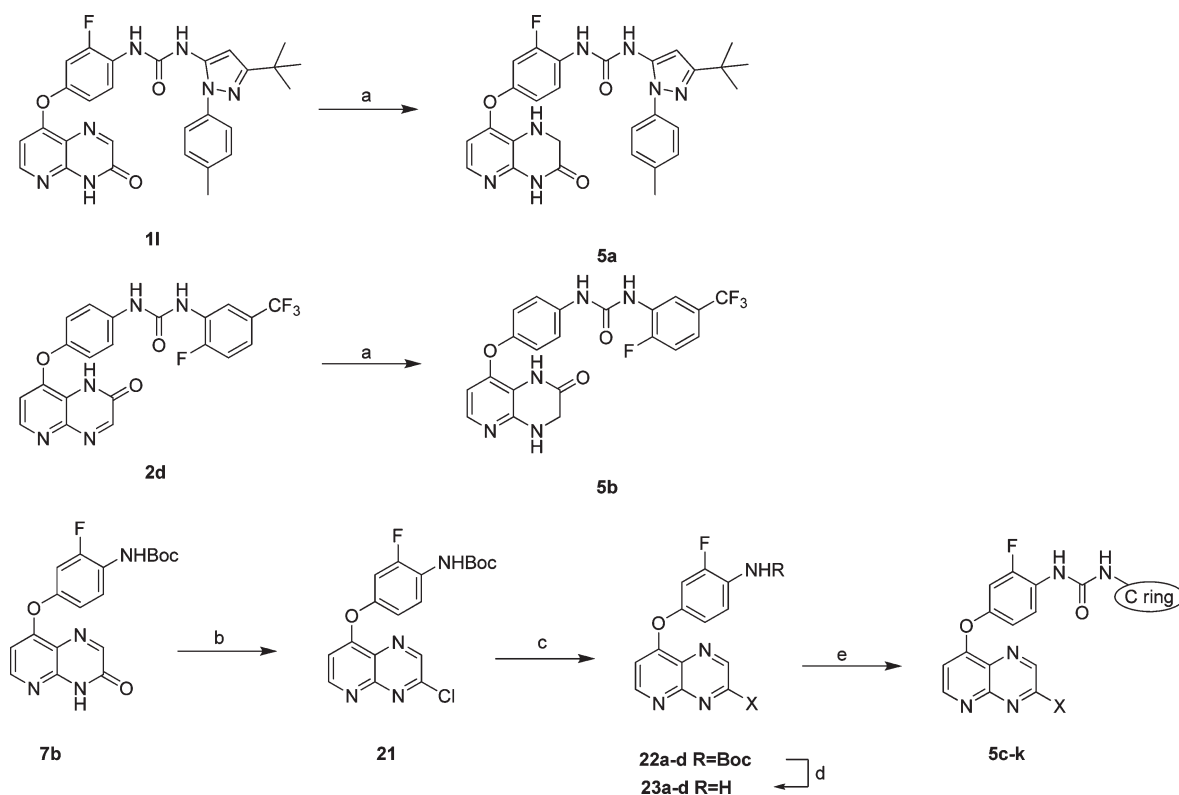
Enzymatic and cellular potencies of the target compounds were evaluated using three previously described *in vitro* assays.^{12,13} In brief, the enzymatic assay measures the IC_{50} of purified $^{\text{V600E}}$ BRAF (IC_{50} , $^{\text{V600E}}$ BRAF) *in vitro*, whereas the other two cellular assays assess the inhibition IC_{50} of the formation of phosphoERK and the proliferation GI_{50} . We previously discussed how the concordance between pERK IC_{50} and SRB GI_{50} values, which is observed throughout the series, provides evidence for the hypothesis that our

compounds inhibit cell growth through inhibition of the ERK pathway, thus suggesting that the observed activity is not due to off-target effects on proliferation but to BRAF inhibition.^{13,15}

The focus of the current work was the identification of effective novel A ring as hinge binders. The SAR analysis was then extended to probe the effects on activity of structural diversity on the B–C ring system, including the change from para to meta substitution pattern on the B ring. Finally, the PK properties of some of the most effective and representative compounds are presented.

Selection of A Ring Fragments. The influence of the structure of ring A on the activity of the compounds in the assays was initially evaluated on compounds bearing a 3-fluoro substituted B-ring connected through a urea linker to a 2-fluoro-5-(trifluoromethyl)phenyl ring C. The benchmark compound for this study is **21r** from ref 13, in which the same B/C ring system is connected to a pyridoimidazolone A ring. The results are summarized in Table 1.

A clear observation from Table 1 is that pyridopyrazin-3(4*H*)-one compounds **1a–d** have both enzymatic and cellular values that are improved or comparable to those of our benchmark compound. The presence of an amino group at the 2 position of the pyrazinone ring leads to a slight decrease in enzymatic activity (compare **1c** and **1a**), while the presence of a lipophilic methyl group in the same position leads to a 2-fold improvement in cellular activity (compare **1b** and **1a**). More strikingly, pyridopyrazin-2(1*H*)-one compounds are noticeably less active than their pyridopyrazin-3(4*H*)-one counterparts on both the enzymatic and cellular assays. The difference in enzymatic activity is more marked between pyrazinone and methyl pyrazinone compounds (compare **1a,b** and **2a,b**) than between aminopyrazinone compounds (compare **1c** with **2c**). Compound **1d**, with two lactam groups, has the same level of activity as pyridopyrazin-3(4*H*)-one compounds **1a–c**. With the exception of compound **3e**, which exhibits a 100-fold decrease in activity with respect to the parent compound **21r** from ref 13, compounds with five-membered heterocycles fused with the pyridine ring show only a slight decrease in both the enzymatic and cellular potencies and generally exhibit an activity that is between those of the related pyridopyrazin-3(4*H*)-one and pyridopyrazin-2(1*H*)-one compounds.

Scheme 4. Derivatization of Pyridopyrazinone Compounds^a

^aReagents and conditions: (a) NaBH₄, dry EtOH; (b) *N*-chlorosuccinimide, PPh₃, dry 1,4-dioxane, Ar, reflux; (c) X = methylpiperazine; *N*-methylpiperazine, dry CH₂Cl₂, Ar, room temp. X = dimethylamino: Me₂NH (2 M in THF), dry THF, 0 °C to room temp. X = morpholino: morpholine, dry CH₂Cl₂, Ar, room temp. X = methylamino: CH₃NH₂ (2 M in THF), dry THF, room temp; (d) 1 M TBAF in THF, reflux; (e) Isocyanates, dry DMSO, Ar atm, room temp.

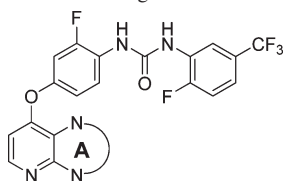
This behavior is consistent with our postulated mode of binding, as higher affinity for the BRAF enzyme is to be expected from compounds bearing an H-bond donor group at N4, next to the pyridine nitrogen, which allows for the formation of a second H-bond with the Cys532 backbone carbonyl group. This explains the difference in activity between compounds **1a–d**, which can form a second H-bond with the hinge through the lactam moiety, and compounds **2a–c**, which are unable to form the H-bond through the endocyclic imine group in position 3. Compounds **3a–d** show intermediate activities, since, as discussed above, the geometry of the five-membered ring leads to the formation of a less favorable H-bond with the backbone.

This model is further validated by the chemical modification of some pyridopyrazinone compounds. When the endocyclic double bond of pyridopyrazin-2(1*H*)-one compound **2d** is reduced, the enzymatic activity of the resulting compound **5a** is improved from 1.29 μM to 54 nM (compare **2d** and **5a** in Table 2). Conversely, when the same reaction is carried out on pyridopyrazin-3(4*H*)-one compound **1l** to give reduced compound **5b**, the two inhibitors show very close activities (compare **1l** and **5b** in Table 2).

Variation of the B–C Fragment. After identifying suitable new A-ring fragments of the inhibitors, we focused on connecting the new A rings to a variety of B–C ring fragments similar to those reported in previous studies (see Table 2 for synthesized compounds).^{12–15} Compounds **2ad** and **2z** from ref 15, the most active inhibitors from the previous series and their activities, are reported in Figure 3 for comparison.

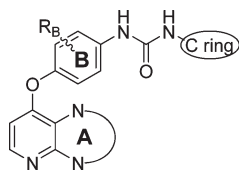
The SAR observation proposed above is also valid for the compounds in Table 2; inhibitors with substituted or unsubstituted pyridopyrazin-3(4*H*)-one A rings are consistently more active than their pyridopyrazin-2(1*H*)-one counterparts on both enzymatic and cellular assays, generally one order of magnitude or greater (e.g., compare **1e** with **2d**, **1n** with **2k**, **1p** with **2l**, and **1v** with **2o**). As observed for the pyridoimidazolone-based compounds,¹⁵ the introduction of 3-*tert*-butyl-1-phenyl-1*H*-pyrazole or a 3-*tert*-butyl-1-*p*-tolyl-1*H*-pyrazole group as C-ring leads to an increase of potency in the cell-based pERK and the SRB cell proliferation assays.

The combination of some of the new A ring moieties with the most active B–C ring fragments that had been previously reported led to a series of compounds with cellular activity at the single-digit nanomolar level, for example, compounds **1s–u** (Table 2), a marked improvement with respect to the most effective inhibitors previously reported. A similar improvement in cellular activity is not observed for compounds **3f–g**, which feature a dimethylaminoimidazole and a benzotriazole group fused to the pyridine ring, respectively, and to a lesser extent for compound **3h**, featuring an imidazolethiol moiety. A possible explanation for the discrepancy between this behavior and the other A-rings investigated can be ascribed to the polarity of the benzotriazole and dimethylaminoimidazole groups, as polar moieties are known to impede the transport of compounds through the cell membrane. As already observed, all other factors being equal, the potency of the inhibitors increases in the order phenyl < naphthyl ~ 3-F-phenyl < 3-MeS-phenyl.^{13,15}

Table 1. Comparison of the Potencies of Inhibitors with Different A-Rings^a

	A	BRAF IC₅₀ (μM)	p-ERK IC₅₀ (μM)	SRB GI₅₀ (μM)
21r ref 13		0.007	1.29	1.15
1a		0.004±0.000	0.78±0.23	1.3 1.13 - 1.49
2a		0.076±0.015	69	1.8 1.65 - 2.01
1b		0.003±0.000	0.59±0.08	0.85 0.72 - 1.0
2b		0.258±0.058	20±2	2.7 2.11 - 3.56
1c		0.030±0.009	1.55±0.07	1.55 1.32 - 1.68
2c		0.168±0.033	9.9±0.7	6.5 5.80 - 7.33
1d		0.005±0.001	0.60±0.07	1.45 1.2 - 1.74
3a		0.069±0.012	24±5	39.0 38.5 - 50.2
3b		0.042±0.006	8.5±1.2	4.85 3.37-6.99
3c		0.017±0.004	13±3	0.97 0.85 - 1.11
3d		0.025±0.003	6±0.3	0.16 0.11 - 0.24
3e		0.73±0.17	>10	1.40 1.23 - 1.60

^aWhere errors are lower than 10–3 μM, the error values are reported as 0.000.

Table 2. Comparison of the Potencies of Inhibitors with Different Combinations of A-, B-, and C-Rings

	A	B	C ring	BRAF IC ₅₀ (μ M)	pERK IC ₅₀ (μ M)	SRB GI ₅₀ (μ M)
1e				0.011±0.002	4.89±1.01	9.1 8.08- 10.20
1f				0.021±0.003	5.2±1.0	3.19 2.81 - 3.62
1g				0.252±0.016	0.096±0.036	0.062 0.58 - 0.76
1h				0.006±0.002	0.66±0.12	1.3 1.12 - 1.50
1i				0.017±0.001	0.62±0.12	0.76 0.66 - 0.89
1j				0.190±0.021	0.273±0.016	0.299 0.25 - 0.30
1k				0.32±0.22	0.011±0.007	0.008 0.006 - 0.011
1l				0.064±0.008	0.024±0.012	0.015 0.009 - 0.027
1m				0.090±0.044	0.075±0.008	0.079 0.067 - 0.095
1n				0.004±0.002	0.187±0.038	0.118 0.097 - 0.144

Table 2. Continued

	A	B	C ring	BRAF IC₅₀ (μ M)	pERK IC₅₀ (μ M)	SRB GI₅₀ (μ M)
1o				0.003±0.001	0.59±0.16	0.22 0.20 - 0.25
1p				0.004±0.002	0.195±0.032	0.096 0.088 - 0.106
1q				0.002±0.001	0.55±0.06	0.19 0.151 - 0.251
1r				0.002±0.000	0.097±0.015	0.225 0.132 - 0.382
1s				0.020±0.002	0.003±0.001	0.004 0.004 - 0.005
1t				0.019±0.004	0.005±0.002	0.001 0.0003 - 0.0036
1u				0.024±0.003	0.006±0.002	0.003 ND
1v				0.004±.001	0.062±0.008	0.036 0.031 - 0.043
1w				0.005±0.001	0.049±0.002	0.015 0.006 - 0.043
1x				0.134±0.025	>10	>10
1y				0.077±0.021	0.008±0.002	0.105 0.088 - 0.127
1z				0.067±0.022	0.008±0.001	0.057 0.051 - 0.064

Table 2. Continued

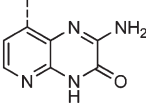
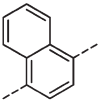
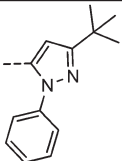
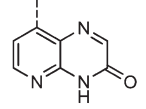
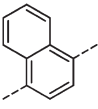
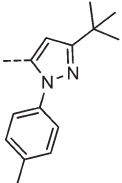
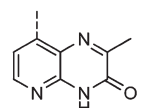
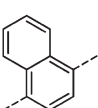
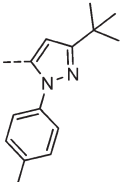
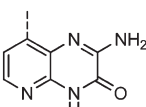
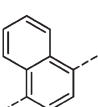
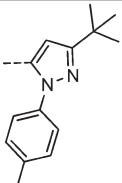
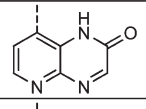
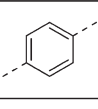
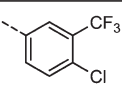
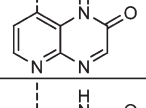
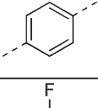
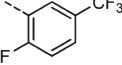
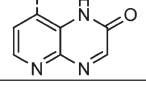
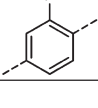
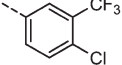
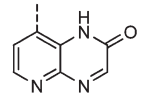
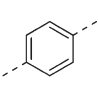
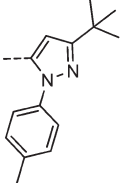
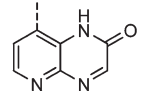
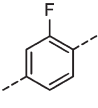
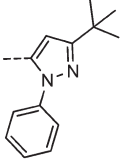
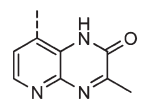
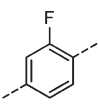
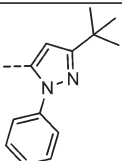
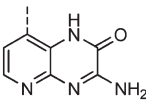
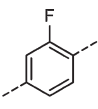
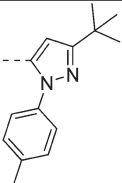
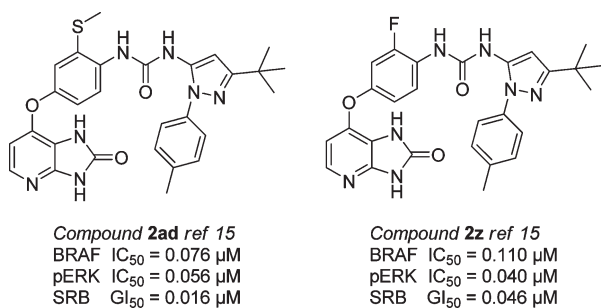
	A	B	C ring	BRAF IC₅₀ (μ M)	pERK IC₅₀ (μ M)	SRB GI₅₀ (μ M)
1aa				0.085±0.000	0.007±0.001	0.009 0.002 - 0.048
1ab				0.080±0.008	0.010±0.000	0.08 0.059 - 0.108
1ac				0.099±0.031	0.005±0.002	0.075 0.059 - 0.096
1ad				0.15±0.06	0.0070±0.002	0.077 ND
2d				0.133±0.021	>100	8.8 7.8 - 9.8
2e				1.29±0.035	4.2	4.0 3.84 - 4.2
2f				0.059±0.007	16±2	3.9 ND
2g				2.29±0.24	0.634±0.046	0.67 0.051 - 0.075
2h				0.94±0.09	0.65±0.119	0.94 0.782 - 1.138
2i				8.5±1.2	0.39±0.06	0.43 0.38 - 0.49
2j				0.222±0.028	0.070±0.008	0.128 0.100 - 0.160

Table 2. Continued

	A	B	C ring	BRAF IC₅₀ (μ M)	pERK IC₅₀ (μ M)	SRB GI₅₀ (μ M)
2k				0.071±0.015	3.99±0.15	4.3 4.0 - 4.6
2l				0.246±0.061	6.6±0.6	5 4.7 - 5.2
2m				0.45±0.05	0.101±0.025	0.027 0.022 - 0.033
2n				0.084±0.021	2.07±0.27	0.486 0.410- 0.530
2o				0.108±0.010	3.4±0.1	8.5 7.1 - 10.1
2p				0.043±0.019	0.229±0.017	0.204 0.161 - 0.257
2q				1.08±0.13	8.5±0.3	10 8.1 - 12.4
2r				0.264±0.027	0.048±0.008	0.073 0.058 - 0.092
2s				3.0±0.7	0.141±0.009	0.095 0.072 - 0.124
2t				0.405±0.049	0.036	0.018 ND
2u				17±2	0.176±0.011	1.5 0.7 - 3.0
3f				1.67±0.05	1.70±0.37	0.574 0.506 - 0.649

Table 2. Continued

	A	B	C ring	BRAF IC ₅₀ (μ M)	pERK IC ₅₀ (μ M)	SRB GI ₅₀ (μ M)
3g				1.37 \pm 0.16	3.1 \pm 0.6	1.98 1.4 - 2.5
3h				0.31 \pm 0.03	0.055 \pm 0.003	0.154 0.056 - 0.171
5a				0.054 \pm 0.006	3.5 \pm 1.3	1.69 1.50- 1.90
5b				0.051 \pm 0.006	0.011 \pm 0.001	0.034 0.025 - 0.046

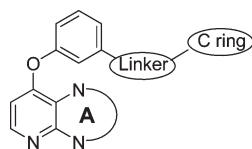
Figure 3. Structural formulas and biological data of compounds **2ad** and **2z** from ref 15.

Extension to the Meta-Scaffold. We recently reported the synthesis of BRAF inhibitors in which the aromatic middle ring connects to the hinge binder and the allosteric pocket binder in a meta substitution pattern.¹⁴ Compounds with this scaffold show low-nanomolar level of inhibition on enzymatic assays and show inhibition on cellular assays in the high nanomolar range. Introduction of the new A-rings on the meta scaffold has led to the synthesis of compounds **4a–n**, whose activity is summarized in Table 3, which also includes the relevant counterparts from ref 14. In this case, the activity of pyridopyrazin-3(4*H*)-one compounds is generally comparable with those of the parent compounds. The noteworthy exception is of the cellular activity of pyrazole compounds bearing an urea linker, whose potency is enhanced by the presence of the pyridopyrazin-3(4*H*)-one fragment, leading to compounds with activities in the 100 nM range on pERK and on SRB assays (compare **4c**, **4e**, and **4g** with compounds **27** and **26** from ref 14).

Introduction of Water-Soluble Groups onto A Ring Fragments. We describe above how the reactivity of the pyridopyrazinone fragment allows the introduction of solubilizing groups on the A ring through its conversion to a pyridochloropyrazine followed by a nucleophilic aromatic substitution. The activities of the resulting compounds are summarized in Table 4. Predictably, given the removal of an H-bond donor from the hinge binder, the activities of these compounds are markedly lower than those of their pyridopyrazin-3(4*H*)-one counterparts (e.g., compare **5c**, **5e**, **5g** with **1a** and compare **5i** with **1l**) and in line with those of pyridopyrazin-2(1*H*)-one compounds (e.g., compare **5c**, **5e**, **5g** with **2a** and compare **5d**, **5f**, **5h** with **2h**).

Kinase and Cellular Selectivity. We previously reported how elaboration on the B-ring confers a remarkable selectivity profile, particularly in the case of compounds with meta-substituted B-rings.^{13,14} To evaluate the effect of the new hinge binders on selectivity, compounds **1p** and **4e**, representing both the para and the meta scaffold, were submitted to the MRC National Centre for Protein Kinase Profiling²⁰ for the assessment of their activity at a single concentration of 1 μ M in a panel of \sim 80 protein kinases (see Table 1 in Supporting Information for full results). As shown in Figure 4, the compounds inhibit only a few kinases in the panel, with SRC, LCK, and p38 being common hits between the two panels, thus confirming the selectivity of this series.

Selectivity of the series versus ^{WT}BRAF can be evaluated by comparing the in-house IC₅₀ versus ^{V600E}BRAF of compounds **1a** and **4e** with the corresponding ^{WT}BRAF results obtained by Invitrogen. Compound **1a** has a ^{WT}BRAF IC₅₀ of 83 nM and a ^{V600E}BRAF IC₅₀ of 4 nM, and **4e** has a ^{WT}BRAF IC₅₀ of 87 nM and a ^{V600E}BRAF IC₅₀ of 918 nM. The differential correlates well with the ratio between

Table 3. Comparison of the Potencies of Inhibitors with Different A-Rings and a Meta Substitution Pattern

	A ring	Linker/C ring	BRAF IC ₅₀ (μ M)	pERK IC ₅₀ (μ M)	SRB GI ₅₀ (μ M)
23 ref 14			0.026	12	1.60
4a			0.041±0.017	10±2	10 8.9 - 11.5
4b			0.105±0.021	>100	6.1 4.8 - 7.6
27 ref 14			0.089	1.33	1.00
4c			0.058±0.011	0.28±	0.17 0.13 - 0.23
4d			0.64±0.16	1.7±0.3	1.6 1.4 - 1.75
26 ref 14			0.128	0.830	0.705
4e			0.087±0.009	0.274±0.038	0.19 0.17 - 0.21
4f			0.58±0.26	0.78±0.20	0.345 0.297 - 0.401
4g			0.132±0.019	0.069±0.007	0.069 0.018 - 0.262

Table 3. Continued

	A ring	Linker/C ring	BRAF IC ₅₀ (μ M)	pERK IC ₅₀ (μ M)	SRB GI ₅₀ (μ M)
39 ref 14			0.014	7.56	1.00
4h			0.021±0.005	4.0±0.6	9.9 7.7 - 12.8
4i			0.306±0.069	37	6.8 6.6 - 7.1
4j			0.024±0.004	6.6±1.2	6.7 5.9 - 7.7
48 ref 14			0.017	3.50	1.83
4k			0.007±0.002	0.85±0.25	1.7 ND
4l			0.034±0.006	3.5±0.7	2.54 2.40 - 2.70
4m			0.010±0.006	1.43±0.35	0.89 0.77 - 1.03
87 ref 14			0.356	1.09	9
4n			0.87±0.17	5.0±2.3	2 1.7 - 2.4

the $K_{m(ATP)app}$ values of WT BRAF and V600E BRAF,²¹ suggesting similar affinities (K_i) of the series for the mutant and wild-type form of the enzyme.

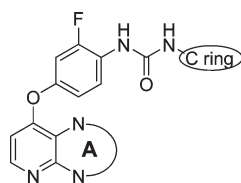
The selectivity of compound **4e** toward BRAF mutant cell lines was also assessed by comparing its SRB GI₅₀ values on the WM266.4 mutant BRAF melanoma cell line and the WM1361 (BRAF wild type/NRAS mutant) and the D24 (BRAF/NRAS wild type) cell lines. The results are presented in Figure 5 and show that **4e** is 60- and 130-fold selective toward the WM1361 and D24 cell line, respectively, supporting evidence that our proposed mechanism of action is through the inhibition of oncogenic BRAF.

PK Properties. The oral bioavailability (F), half-life ($t_{1/2}$), and maximum concentrations (C_{max}) of some of the inhibitors were determined in vivo. The results are presented in Table 5.¹⁴

It is worth noting that diketo compound **1m** shows lower F and peak concentration C_{max} with respect to its unsubstituted analogue. These poor PK parameters could be explained by the presence on the A ring of an additional

H-bond group. Compounds with a naphthyl B-ring and phenyl C-ring have poor F and peak concentrations (compounds **1y**, **1z**), while compound **3h** has similar PK parameters to its pyridoimidazolone analogue **2z** from ref 15. It was observed¹⁵ that phenyl C rings have a detrimental effect on oral bioavailability; indeed, compound **1v**, which bears both a naphthyl B ring and a phenyl C ring, has particularly poor PK parameters and no appreciable half-life. Meta compound **4e**, with a tolylpyrazole C ring, shows an improved F compared with its phenylpyrazole analogue **4c**.

Besides compound **4e**, many of the compounds assessed exhibit concentrations well above their GI₅₀ values (some over 100 000-fold) for extended periods following oral administration. In particular, compound **1t** shows a high oral bioavailability along with a long half-life, maintaining a concentration greater than the GI₅₀ for over 24 h, and represents an improvement in PK properties compared to the inhibitors previously reported.¹⁵ This, combined with the potency of the compound, suggests potential for therapeutic efficacy in vivo in human tumor xenograft models.

Table 4. Comparison of the Potencies of Inhibitors Featuring Solubilizing Groups on the A-Ring

	A	C ring	BRAF IC₅₀ (μM) ^a	pERK IC₅₀ (μM)	SRB GI₅₀ (μM)
5c			0.118±0.019	16±6	0.12 0.054 - 0.268
5d			4.1±0.9	0.75±0.12	0.417 0.253 - 0.492
5e			0.22±0.07	20±12	55 44.8 - 68.0
5f			>10	1.7±0.6	1.1 1.0 - 1.2
5g			0.097±0.013	3.8±1.2	1.12 0.8 - 1.6
5h			8.2±1.2	0.75±0.08	0.428 0.353 - 0.517
5i			>10	0.28±0.04	0.235 0.131 - 0.422
5j			0.107±0.042	45±11	48 ND

Conclusions

Potential improved mutant BRAF inhibitors bearing alternative hinge binders (A-rings) have been synthesized. This study identified 2-substituted pyridopyrazin-3(4*H*)-one groups as optimized A rings, which we postulate form enhanced interactions with the hinge region. The combination of this new scaffold with substituted phenyl B rings and 3-*tert*-butyl-1-aryl-1*H*-pyrazoles C rings leads to inhibitors exhibiting single-digit nanomolar potencies on both enzymatic and cellular assays, with an improvement compared to the most potent compounds reported thus far. One of the new compounds shows an oral bioavailability of over 70% in mouse and maintains a concentration above the GI₅₀ for 24 h after administration, which suggests the potential to exhibit therapeutic efficacy *in vivo* in human tumor xenograft models.

Experimental Section

Materials and Methods. Starting materials, reagents, and solvents for reactions were reagent grade and used as purchased. *tert*-butyl 4-(2,3-diaminopyridin-4-yloxy)-2-fluorophenylcarbamate,¹³ *tert*-butyl 4-(2,3-diaminopyridin-4-yloxy)phenylcarbamate,¹² *tert*-butyl 4-(2,3-diaminopyridin-4-yloxy)-2-(methylthio)phenylcarbamate,¹³ *tert*-butyl 4-(2,3-diaminopyridin-4-

yloxy)naphthalen-1-ylcarbamate,¹³ *tert*-butyl 4-(2-amino-3-nitropyridin-4-yloxy)-2-fluorophenylcarbamate,¹³ *tert*-butyl 4-(2-amino-3-nitropyridin-4-yloxy)-2-(methylthio)phenylcarbamate,¹³ *tert*-butyl 3-(3-oxo-3,4-dihydropyrido[2,3-*b*]pyrazin-8-yloxy)-phenylcarbamate,¹⁴ and 3-*tert*-butyl-1-phenyl-1*H*-pyrazol-5-amine¹⁴ were synthesized according to described procedures. Chromatography solvents were HPLC grade and were used without further purification. Reactions were monitored by thin layer chromatography (TLC) analysis using Merck silica gel 60 F-254 thin layer plates. Flash column chromatography was carried out on Merck silica gel 60 (0.015–0.040 mm) or in disposable Isolute Flash Si and Si II silica gel columns. Preparative TLC was performed on either Macherey-Nagel [809 023] precoated TLC plates SIL G-25 UV₂₅₄ or Analtech [2015] precoated preparative TLC plates, 2000 μm with UV₂₅₄. LCMS analyses were performed on a Micromass LCT/Water's Alliance 2795 HPLC system with a Discovery 5 μm, C18, 50 mm × 4.6 mm i.d. column from Supelco at 22 °C using the following solvent systems: solvent A, methanol; solvent B, 0.1% formic acid in water at a flow rate of 1 mL/min. Gradient started with 10% A/90% B from 0 to 0.5 min and then from 10% A/90% B to 90% A/10% B from 0.5 to 6.5 min and continued at 90% A/10% B to 10 min. From 10 to 10.5 min the gradient reverted back to 10% A/90% B where the concentrations remained until 12 min. UV detection was at 254 nm, and ionization was positive or negative ion electrospray. The molecular weight scan range was 50–1000. Samples were supplied as 1 mg/mL in DMSO or methanol with 3 μL injected on a partial loop fill. NMR spectra were recorded in DMSO-*d*₆ on a Bruker DPX 250 MHz or a Bruker Advance 500 MHz spectrometer. Chemical shifts (δ) are given in ppm and are referenced to residual, not fully deuterated solvent signal (i.e., DMSO-*d*₅). Coupling constants (*J*) are given in Hz. The purities of the final compounds described here were determined by HPLC as described above and are 95% or higher unless stated otherwise.

Docking. Inhibitors were docked on BRAF (PDB code UWH) using GOLD, version 3.1.1.²² In order to prepare the receptor for docking, the crystal structure was protonated using

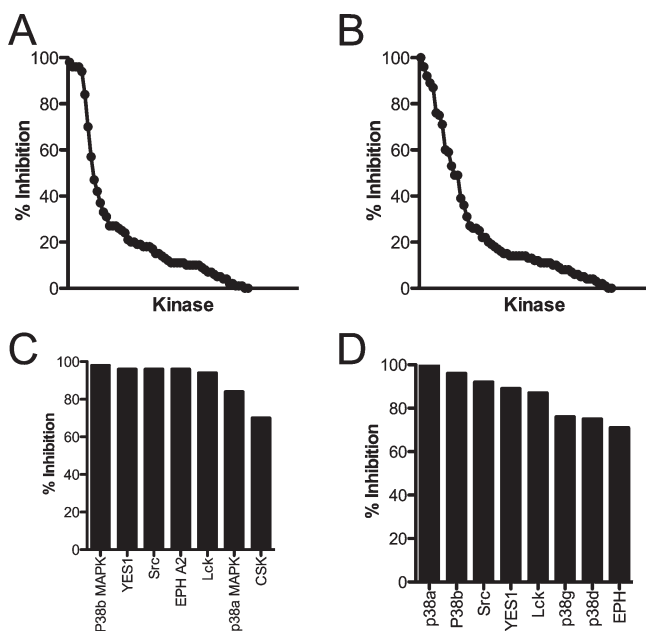


Figure 4. Kinase selectivity of compounds **1p** (A) and **4e** (B) tested at 1 μM against a panel of ~80 kinases at the MRC National Centre for Protein Kinase Profiling. The kinases inhibited by > 70% are presented: (C) **1p** and (D) **4e**.

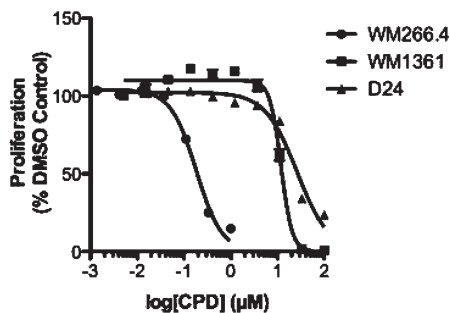


Figure 5. Antiproliferative effect of **4e** in WM266.4 (BRAF mutant), WM1361 (NRAS mutant), and D24 (BRAF/NRAS wildtype) as determined by SRB assay. The selectivity index is calculated by expressing the GI₅₀ values relative to the GI₅₀ value for WM266.4 cells.

Table 5. Pharmacokinetic Data for Selected Compounds, Based on Plasma Levels after a 10 mg/kg Single Dose po

compd ^a	<i>F</i> , %	<i>t</i> _{1/2} , h ^b	<i>C</i> _{max} , nM ^c
1g	17	6.3 (24)	31853 (0.5, 510)
1l	24	5.9 (24)	33640 (3, 2240)
1m	1	5.4 (> 18)	5536 (3, 70)
1t	71	7.9 (24)	101199 (3, 101200)
1v	4	(6)	316 (3, 9)
1y	7	1.7 (11)	14165 (0.25, 130)
3h	13	3.3 (24)	11652 (3, 76)
4c	6	1.4 (6)	29543 (0.5, 170)
4e	27	4.0 (24)	26989 (0.5, 142)

^a 10 mg/kg single dose po in mouse. ^b In parentheses the number of hours the concentration of a compound is above its GI₅₀ after oral administration. ^c In parentheses the *t*_{max} [h] and the ratio between the plasma concentration of the compound and its GI₅₀ at *t*_{max} after oral administration.

Cell Line	GI ₅₀ (μM)	Selectivity Index
WM266.4	0.2	1
WM1361	12	60
D24	26	130

the Protonate3D tool of MOE, and the ligand and water molecules were then removed. The active site was defined using a radius of 10 Å from the backbone oxygen atom of Asp594 of the ATP binding pocket. Partial charges of the ligands were derived using the Charge-2 CORINA 3D package in TSAR 3.3 and their geometries optimized using the COSMIC module of TSAR. Ten docking solutions were generated per docking run with GOLD, and the best three were stored for analysis.

X-ray Crystallographic Analysis. Crystallographic data for compound **8b** have been deposited with the Cambridge Crystallographic Data Center as Supplementary Publication. Copies of the data can be obtained, free of charge, on application to CCDC, 12 Union Road, Cambridge CH21EZ, U.K. (fax, +44 1223 336 033; e-mail, deposit@ccdc.cam.ac.uk), CCDC deposition number 778231. Figure 1 (in Supporting Information) shows an ORTEP-3 diagram of **8b**.

Biological Assays. ^{V600E}BRAF Kinase Assay and SRB IC₅₀ for BRAF Inhibitors. These assays have been described by Niculescu-Duvaz et al.¹²

pERK Kinase Assay. This assay has been described by Ménard et al.¹³

Pharmacokinetics. Female BALB/cAnNCrl mice at least 6 weeks of age were used for the PK analysis except for the intravenous administration of **1m**, which was carried out with female CrI:CD1-Foxn1nu mice bearing V600E mutant BRAF WM266.4 tumor xenografts. The mice were dosed intravenously (2 mg/kg, equivalent to ~4 μmol/kg, 10 mL/kg, in DMSO/Tween-20/water 10:1:89 v/v) or orally by gavage. Samples were taken at seven or eight time-points between 5 min and 18 or 24 h for the intravenous route and at six or eight time-points between 15 min and 18 or 24 h for the oral route. Three mice were used per time-point per route. They were placed under halothane or isoflurane anesthesia, and blood for plasma preparation was taken by terminal cardiac puncture into heparinized syringes. Plasma samples were snap frozen in liquid nitrogen and then stored at -70 °C prior to analysis. All procedures involving animals were performed in accordance with national Home Office regulations under the Animals (Scientific Procedures) Act 1986 and within guidelines set out by the Institute's Animal Ethics Committee and the United Kingdom Coordinating Committee for Cancer Research's ad hoc Committee on the Welfare of Animals in Experimental Neoplasia.²³

Method 2: Synthesis of the 2-Substituted Pyrido[2,3-*b*]pyrazin-3(4*H*)-one and 3-Substituted Pyrido[2,3-*b*]pyrazin-2(1*H*)-one Regioisomers. To a solution of the appropriate *tert*-butyl 4-(2,3-diaminopyridin-4-yloxy-2-phenylcarbamate in dry EtOH were added consecutively molecular sieves (3 Å) and ethyl glyoxylate (3.6 mL of a 50% solution in toluene, 1.7 equiv). The solution was stirred at room temperature until the starting material was consumed (monitored by TLC). Then the mixture was evaporated to dryness and subjected to column chromatography (elution with CH₂Cl₂ to EtOAc/CH₂Cl₂ (1/2, v/v toward 1/1, v/v).

***tert*-Butyl 4-(3-Oxo-3,4-dihydropyrido[2,3-*b*]pyrazin-8-yloxy)-phenylcarbamate **7a** and *tert*-Butyl 4-(2-Oxo-1,2-dihydropyrido[2,3-*b*]pyrazin-8-yloxy)phenylcarbamate **8a**.** Method 2 was used overnight with *tert*-butyl 4-(2,3-diaminopyridin-4-yloxy)-phenylcarbamate¹² (0.86 g, 2.71 mmol) to provide **7a** (0.200 g, 21% yield) and **8a** (0.430 g, 45% yield).

***tert*-Butyl 4-(3-Oxo-3,4-dihydropyrido[2,3-*b*]pyrazin-8-yloxy)-phenylcarbamate **7a**.** ¹H NMR δ (in CDCl₃): 1.54 (s, 9H, ^tBu), 6.55 (d, 1H, *H*_{Py}, *J* = 5.5), 6.67 (bs, 1H, *H*_{arom}), 7.14 (d, 2H, *H*_{arom}, *J* = 8.5), 7.49 (d, 2H, *H*_{arom}, *J* = 8.5), 8.36 (s, 1H, *NH*Boc), 8.46 (d, 1H, *H*_{Py}, *J* = 5.5), 12.88 (bs, 1H, *NH*). LCMS *m/z*: 367 (M + H, 100).

***tert*-Butyl 4-(2-Oxo-1,2-dihydropyrido[2,3-*b*]pyrazin-8-yloxy)-phenylcarbamate **8a**.** ¹H NMR δ (in CDCl₃): 1.49 (s, 9H, ^tBu), 6.76 (d, 1H, *H*_{Py}, *J* = 5.4), 7.15 (d, 2H, *H*_{arom}, *J* = 9.0), 7.57 (d, 2H, *H*_{arom}, *J* = 9.0), 8.32 (d, 1H, *H*_{Py}, *J* = 5.0), 8.40 (s, 1H, *H*_{arom}), 9.44 (bs, 1H, *NH*Boc), 12.54 (bs, 1H, *NH*). LCMS: *m/z* 367 (M + H, 100).

Method 4: Introduction of the Linker/C Ring. A solution of appropriate regioisomer (1 mmol) in dry DMSO (1 mL) under Ar was treated with the isocyanate (1 mmol), and the solution was stirred at room temperature. After 3 h, the solution was diluted with H₂O and the precipitate was isolated by filtration.

1-(2-Fluoro-4-(3-oxo-3,4-dihydropyrido[3,2-*b*]pyrazin-8-yloxy)-phenyl)-3-(2-fluoro-5-(trifluoromethyl)phenyl)urea **1a.** Method 4 was used with 4-(4-amino-3-fluorophenyl)pyridopyrazine-3(4*H*)-one **9b** and 1-fluoro-2-isocyanato-4-(trifluoromethyl)-benzene (yield = 80%). ¹H NMR δ: 6.67 (d, 1H, *H*_{Py}, *J* = 5.5), 7.08 (m, 1H, *H*_{arom}), 7.34 (m, 1H, *H*_{arom}), 7.40 (m, 1H, *H*_{arom}), 7.51 (m, 1H, *H*_{arom}), 8.17 (s, 1H, *H*_{arom}), 8.23 (t, 1H, *H*_{arom}, *J* = 8.1), 8.38 (d, 1H, *H*_{Py}, *J* = 5.5), 8.64 (m, 1H, *H*_{arom}), 9.20 (s, 1H, *NH*), 9.35 (s, 1H, *NH*), 12.91 (br s, 1H, *NH*Ar). ¹⁹F NMR δ: -60.8, -124.0, 125.2. LCMS: *m/z* 478 (M + H, 100, 5.04 min). HRMS (3.38 min): *m/z* calcd for C₂₁H₁₃F₅N₅O₃ [(M + H)⁺] 478.0933; found 478.0935.

1-(3-*tert*-Butyl-1-*p*-tolyl-1*H*-pyrazol-5-yl)-3-(2-(methylthio)-4-(3-oxo-3,4-dihydropyrido[2,3-*b*]pyrazin-8-yloxy)phenyl)urea **1t.** Method 4 was used with 8-(4-amino-3-(methylthio)phenoxy)pyrido[3,2-*b*]pyrazin-3(4*H*)-one **9d** and 3-*tert*-butyl-5-isocyanato-1-*p*-tolyl-1*H*-pyrazole. The title compound (5 mg, 8%) was obtained as a white powder after purification on silica gel (eluent DCM/EtOAc, 1/1, *R*_f = 0.57). ¹H NMR δ: 1.31 (s, 9H, ^tBu), 2.23 (s, 3H, *CH*₃), 2.31 (s, 3H, *SC*H₃), 6.30 (s, 1H), 6.36 (s, 1H), 6.49 (d, 1H, *H*_{Py}, *J* = 5.8), 7.02 (dd, 1H, *H*_{arom}, *J* = 8.9, *J* = 2.7), 7.19 (m, 4H, *H*_{arom}), 7.31 (d, 1H, *H*_{arom}, *J* = 8.3), 7.81 (s, 1H, *NH* or *CH*), 8.16 (d, 1H, *H*_{arom}, *J* = 8.9), 8.26 (s, 1H, *NH* or *CH*), 8.30 (d, 1H, *H*_{Py}, *J* = 5.8), 11.37 (s, 1H, *NH*). LCMS: *m/z* 556 (M + H, 100). HRMS: *m/z* calcd for C₂₉H₂₉N₇O₃S [(M + H)⁺] 556.2125; found 556.2124.

Acknowledgment. We thank Cancer Research UK (Grants C309/A8274 and C107/A10433), the Wellcome Trust, the Institute of Cancer Research, and the Isle of Man Anti-Cancer Association for funding. We thank Dr. Peter N. Horton and Dr. Michael B. Hursthouse of the EPSRC National Crystallography Service (University of Southampton, U.K.) for collection of diffraction data and structure determination of compound **8b**. We are grateful to Neus Cantarino for providing technical assistance, Meirion Richards, Dr. Maggie Liu, and Dr. Amin Mirza for analytical chemistry support and to Professors Julian Blagg and Paul Workman for suggestions, support, and helpful comments. This work was carried out as part of a research collaboration between the Institute of Cancer Research, The Wellcome Trust and Cancer Research U.K. Please note that all authors who are, or have been, employed by The Institute of Cancer Research are subject to a 'Rewards to Inventors Scheme' that may reward contributors to a program that is subsequently licensed.

Supporting Information Available: Experimental details of the synthesis and analytical characterization of all compounds; X-ray diffraction data for compound **8b**; selectivity profile for compounds **1p** and **4e**. This material is available free of charge via the Internet at <http://pubs.acs.org>.

References

- Hanahan, D.; Weinberg, R. A. The hallmarks of cancer. *Cell* **2000**, *100* (1), 57–70.
- Davies, H.; Bignell, G. R.; Cox, C.; Stephens, P.; Edkins, S.; Clegg, S.; Teague, J.; Woffendin, H.; Garnett, M. J.; Bottomley, W.; Davis, N.; Dicks, E.; Ewing, R.; Floyd, Y.; Gray, K.; Hall, S.; Hawes, R.; Hughes, J.; Kosmidou, V.; Menzies, A.; Mould, C.; Parker, A.; Stevens, C.; Watt, S.; Hooper, S.; Wilson, R.; Jayatilake, H.; Gusterson, B. A.; Cooper, C.; Shipley, J.; Hargrave, D.; Pritchard-Jones, K.; Maitland, N.; Chenevix-Trench, G.; Riggins, G. J.; Bigner, D. D.; Palmieri, G.; Cossu, A.; Flanagan, A.; Nicholson, A.; Ho, J. W.; Leung, S. Y.; Yuen, S. T.; Weber, B. L.; Seigler, H. F.; Darrow, T. L.;

- Paterson, H.; Marais, R.; Marshall, C. J.; Wooster, R.; Stratton, M. R.; Futreal, P. A. Mutations of the BRAF gene in human cancer. *Nature* **2002**, *417* (6892), 949–954.
- (3) Garnett, M. J.; Marais, R. Guilty as charged: B-RAF is a human oncogene. *Cancer Cell* **2004**, *6* (4), 313–319.
- (4) Wan, P. T.; Garnett, M. J.; Roe, S. M.; Lee, S.; Niculescu-Duvaz, D.; Good, V. M.; Jones, C. M.; Marshall, C. J.; Springer, C. J.; Barford, D.; Marais, R. Mechanism of activation of the RAF-ERK signaling pathway by oncogenic mutations of B-RAF. *Cell* **2004**, *116* (6), 855–867.
- (5) Hingorani, S. R.; Jacobetz, M. A.; Robertson, G. P.; Herlyn, M.; Tuveson, D. A. Suppression of BRAF(V599E) in human melanoma abrogates transformation. *Cancer Res.* **2003**, *63* (17), 5198–5202.
- (6) Karasarides, M.; Chioleches, A.; Hayward, R.; Niculescu-Duvaz, D.; Scanlon, I.; Friedlos, F.; Ogilvie, L.; Hedley, D.; Martin, J.; Marshall, C. J.; Springer, C. J.; Marais, R. B-RAF is a therapeutic target in melanoma. *Oncogene* **2004**, *23* (37), 6292–6298.
- (7) Hoeflich, K. P.; Gray, D. C.; Eby, M. T.; Tien, J. Y.; Wong, L.; Bower, J.; Gogineni, A.; Zha, J.; Cole, M. J.; Stern, H. M.; Murray, L. J.; Davis, D. P.; Seshagiri, S. Oncogenic BRAF is required for tumor growth and maintenance in melanoma models. *Cancer Res.* **2006**, *66* (2), 999–1006.
- (8) Tsai, J.; Lee, J. T.; Wang, W.; Zhang, J.; Cho, H.; Mamo, S.; Bremer, R.; Gillette, S.; Kong, J.; Haass, N. K.; Sproesser, K.; Li, L.; Smalley, K. S.; Fong, D.; Zhu, Y. L.; Marimuthu, A.; Nguyen, H.; Lam, B.; Liu, J.; Cheung, I.; Rice, J.; Suzuki, Y.; Luu, C.; Settachatgul, C.; Shellooe, R.; Cantwell, J.; Kim, S. H.; Schlessinger, J.; Zhang, K. Y.; West, B. L.; Powell, B.; Habets, G.; Zhang, C.; Ibrahim, P. N.; Hirth, P.; Artis, D. R.; Herlyn, M.; Bollag, G. Discovery of a selective inhibitor of oncogenic B-Raf kinase with potent antimelanoma activity. *Proc. Natl. Acad. Sci. U.S.A.* **2008**, *105* (8), 3041–3046.
- (9) Roberts, P. J.; Der, C. J. Targeting the Raf-MEK-ERK mitogen-activated protein kinase cascade for the treatment of cancer. *Oncogene* **2007**, *26* (22), 3291–3310.
- (10) King, A. J.; Patrick, D. R.; Batorsky, R. S.; Ho, M. L.; Do, H. T.; Zhang, S. Y.; Kumar, R.; Rusnak, D. W.; Takle, A. K.; Wilson, D. M.; Hugger, E.; Wang, L.; Karreth, F.; Loughheed, J. C.; Lee, J.; Chau, D.; Stout, T. J.; May, E. W.; Rominger, C. M.; Schaber, M. D.; Luo, L.; Lakdawala, A. S.; Adams, J. L.; Contractor, R. G.; Smalley, K. S.; Herlyn, M.; Morrissey, M. M.; Tuveson, D. A.; Huang, P. S. Demonstration of a genetic therapeutic index for tumors expressing oncogenic BRAF by the kinase inhibitor SB-590885. *Cancer Res.* **2006**, *66* (23), 11100–11105.
- (11) Schwartz, G. K.; Yazji, S.; Mendelson, D. S.; Dickson, M. A.; Johnston, S. H.; Wang, E. W.; Shannon, P.; Pace, L.; Gordon, M. S. A phase I study of XL281, a potent and selective inhibitor of RAF kinases, administered orally to patients (pts) with advanced solid tumors. *EJC Suppl.* **2008**, *6* (12), 120–120.
- (12) Niculescu-Duvaz, D.; Gaulon, C.; Dijkstra, H. P.; Niculescu-Duvaz, I.; Zambon, A.; Menard, D.; Suijkerbuijk, B. M.; Nourry, A.; Davies, L.; Manne, H.; Friedlos, F.; Ogilvie, L.; Hedley, D.; Whittaker, S.; Kirk, R.; Gill, A.; Taylor, R. D.; Raynaud, F. I.; Moreno-Farre, J.; Marais, R.; Springer, C. J. Pyridoimidazolones as novel potent inhibitors of v-Raf murine sarcoma viral oncogene homologue B1 (BRAF). *J. Med. Chem.* **2009**, *52* (8), 2255–2264.
- (13) Menard, D.; Niculescu-Duvaz, I.; Dijkstra, H. P.; Niculescu-Duvaz, D.; Suijkerbuijk, B. M.; Zambon, A.; Nourry, A.; Roman, E.; Davies, L.; Manne, H. A.; Friedlos, F.; Kirk, R.; Whittaker, S.; Gill, A.; Taylor, R. D.; Marais, R.; Springer, C. J. Novel potent BRAF inhibitors: toward 1 nM compounds through optimization of the central phenyl ring. *J. Med. Chem.* **2009**, *52* (13), 3881–3891.
- (14) Nourry, A.; Zambon, A.; Davies, L.; Niculescu-Duvaz, I.; Dijkstra, H. P.; Menard, D.; Gaulon, C.; Niculescu-Duvaz, D.; Suijkerbuijk, B. M.; Friedlos, F.; Manne, H. A.; Kirk, R.; Whittaker, S.; Marais, R.; Springer, C. J. BRAF inhibitors based on an imidazo[4,5]pyridin-2-one scaffold and a meta substituted middle ring. *J. Med. Chem.* **2010**, *53* (5), 1964–1978.
- (15) Suijkerbuijk, B. M.; Niculescu-Duvaz, I.; Gaulon, C.; Dijkstra, H. P.; Niculescu-Duvaz, D.; Menard, D.; Zambon, A.; Nourry, A.; Davies, L.; Manne, H. A.; Friedlos, F.; Ogilvie, L. M.; Hedley, D.; Lopes, F.; Preece, N. P.; Moreno-Farre, J.; Raynaud, F. I.; Kirk, R.; Whittaker, S.; Marais, R.; Springer, C. J. Development of novel, highly potent inhibitors of V-RAF murine sarcoma viral oncogene homologue B1 (BRAF): increasing cellular potency through optimization of a distal heteroaromatic group. *J. Med. Chem.* **2010**, *53* (7), 2741–2756.
- (16) Liu, Y.; Gray, N. S. Rational design of inhibitors that bind to inactive kinase conformations. *Nat. Chem. Biol.* **2006**, *2* (7), 358–364.
- (17) Routier, S.; Sauge, L.; Ayerbe, N.; Coudert, G.; Merour, J.-Y. A mild and selective method for N-Boc deprotection. *Tetrahedron Lett.* **2002**, *43* (4), 589–591.
- (18) Correa, A.; Tellitu, I.; Dominguez, E.; SanMartin, R. Novel alternative for the N–S bond formation and its application to the synthesis of benzisothiazol-3-ones. *Org. Lett.* **2006**, *8* (21), 4811–4813.
- (19) Sugimoto, O.; Mori, M.; Moriya, K.; Tanji, K.-I. Application of phosphonium salts to the reactions of various kinds of amides. *Helv. Chim. Acta* **2001**, *84* (5), 1112–1118.
- (20) Davies, S. P.; Reddy, H.; Caivano, M.; Cohen, P. Specificity and mechanism of action of some commonly used protein kinase inhibitors. *Biochem. J.* **2000**, *351* (Part 1), 95–105.
- (21) Hatzivassiliou, G.; Song, K.; Yen, I.; Brandhuber, B. J.; Anderson, D. J.; Alvarado, R.; Ludlam, M. J.; Stokoe, D.; Gloor, S. L.; Vigers, G.; Morales, T.; Aliagas, I.; Liu, B.; Sideris, S.; Hoeflich, K. P.; Jaiswal, B. S.; Seshagiri, S.; Koeppen, H.; Belvin, M.; Friedman, L. S.; Malek, S. RAF inhibitors prime wild-type RAF to activate the MAPK pathway and enhance growth. *Nature* **2010**, *464* (7287), 431–435.
- (22) Jones, G.; Willett, P.; Glen, R. C.; Leach, A. R.; Taylor, R. Development and validation of a genetic algorithm for flexible docking. *J. Mol. Biol.* **1997**, *267* (3), 727–748.
- (23) Workman, P.; Balmain, A.; Hickman, J. A.; McNally, N. J.; Rohas, A. M.; Mitchison, N. A.; Pierrepont, C. G.; Raymond, R.; Rowlatt, C.; Stephens, T. C.; et al. UKCCCR guidelines for the welfare of animals in experimental neoplasia. *Lab. Anim.* **1988**, *22* (3), 195–201.